JPEDAV (2014) 35:587–594
DOI: 10.1007/s11669-014-0328-4
1547-7037 ©ASM International

Thermodynamic Description of Ternary Fe-X-P Systems. Part 3: Fe-Mn-P

Jyrki Miettinen and Gueorgui Vassilev

(Submitted March 27, 2014; in revised form June 20, 2014; published online August 12, 2014)

Thermodynamic descriptions of the Fe-Mn-P system and its binary sub-system, Mn-P, are developed in the frame of a new Fe-X-P (X = Al, Cr, Cu, Mn, Mo, Nb, Ni, Si, Ti) database. The thermodynamic parameters of the binary sub-systems, Fe-Mn and Fe-P, are taken from the latest earlier assessments. Those of the Fe-Mn-P and Mn-P systems are optimized in this study using literature experimental thermodynamic and phase equilibrium data. The solution phases of the system are described with the substitutional solution model and the phosphides are treated as stoichiometric phases or semi-stoichiometric phases of the $(A,B)_pC_q$ type described with the two-sublattice model. The formation of a miscibility gap in the liquid phase, at high P-contents is predicted.

Keywords Fe-based systems, Fe-Mn-P system, Fe-X-P systems, phase diagrams, ternary phase diagram, thermodynamic database, thermodynamic modelling

1. Introduction

The current work continues an earlier started project[1,2] for the development of a thermodynamic database of phosphorus containing Fe-X systems. In such a way a simple and compatible thermodynamic database for three-component steels is to be designed. It would provide important and practical input data for thermodynamic-kinetic models simulating their solidification.[3] The first two contributions concern the systems Fe-Cr-P[1] and Fe-Cu-P.[2]

The goal of the current work is to attain, for the first time, thermodynamic optimizations for the Fe-Mn-P and the Mn-P systems. The latter is based on the earlier Mn-P optimization of Miettinen.[4] The adjustable thermodynamic parameters used for the description of the Fe-Mn and the Fe-P phase diagrams are taken from Huang[5] and from Shim et al.,[6] respectively.

2. Phases, Modeling and Data

Detailed descriptions for the substitutional solution and sublattice models and their parameters are available from Ref 7 and in this journal by Ref 1. Thus, abbreviated descriptions of the phases and models are presented only (Table 1). The solution phases (liquid, bcc_A2, fcc_A1, cbcc_A12, cub_A13) are described with the substitutional solution model. Some phosphides are described with the sublattice model (Fe_3P, Fe_2P, Mn_3P) and other phases are treated as stoichiometric (FeP, Mn_3P_2, MnP, white_P).

Complete mutual solubility was assumed between Fe_2P and Mn_2P, in agreement with the experimental data of Ref 8,9, though according to other authors,[10-12] an ordering reaction (at an undetermined temperature) yielding to an orthorhombic structure for compositions $0.31 < x < 0.62$ of $(Fe_{1-x},Mn_x)_2P$[13] was observed.

The experimental studies on the Fe-Mn-P system up to 1988 have been reviewed by Raghavan.[13] Table 2 shows the experimental information[9,14-22] selected in the current optimization for the Mn-P and Fe-Mn-P systems.

3. Results

The thermodynamic description of the Fe-Mn-P system is presented in Table 3. The parameters marked with a reference code were adopted from earlier assessments and those marked with O* or E* were, respectively, optimized or estimated in the current study. By O*, the parameter was optimized using literature experimental data (Table 2) and by E*, the parameter was estimated arbitrarily.

As previously reported,[1] the Gibbs energy expressions of Fe_3P, Fe_2P and FeP have been simplified by changing the reference states of Fe and P from HSER (used by Shim et al.[6]) to bcc-Fe and white P, respectively. In a similar way, the reference states for the Gibbs energy expression for Mn_3P has been changed from cub-Mn and P_2-gas (used by Zaitsev et al.[19]) to bcc-Fe and white P (Table 3). This change has no perceptible influence on the function values.

Further, calculated phase equilibria and thermodynamic quantities have been compared to original experimental data to in order to verify the results. All calculations were carried out with the ThermoCalc software.[24]

Jyrki Miettinen, School of Chemical Technology, Aalto University, Espoo, Finland; and **Gueorgui Vassilev,** Faculty of Chemistry, University of Plovdiv, 24 Tsar Asen str., 4000 Plovdiv, Bulgaria. Contact e-mails: gpvassilev@gmail.com and gpvassilev@uni-plovdiv.bg.

Table 1 Phases and their modeling in the present Fe-Mn-P description

Phase	Modeling
Liquid (L)	(Fe,Mn,P), substitutional, RKM
bcc_A2 (bcc)	(Fe,Mn,P), substitutional, RKM
fcc_A1 (fcc)	(Fe,Mn,P), substitutional, RKM
cbcc_A12 (cbcc)	(Fe,Mn,P), substitutional, RKM
cub_A13 (cub)	(Fe,Mn,P), substitutional, RKM
Fe_3P (dissolving Mn)	$(Fe,Mn)_3(P)$, sublattice, RKM
Fe_2P (extending to Mn_2P)	$(Fe,Mn)_2(P)$, sublattice, RKM
Mn_3P (dissolving Fe)	$(Fe,Mn)_3(P)$, sublattice, RKM
FeP	(Fe)(P), stoichiometric
Mn_3P_2	$(Mn)_3(P)_2$, stoichiometric
MnP	(Mn)(P), stoichiometric
white_P (whi)	(P)

RKM Redlich-Kister-Muggianu expression (excess Gibbs energy model)

Table 2 Experimental data applied in the current optimization of the Mn-P and Fe-Mn-P systems

System	Experimental data	Reference
Mn-P	Phase equilibria of the phase diagram	[14]
	Activity of Mn and P in liquid alloys, at 1320 °C	[15,16]
	Gibbs energies of formation of Mn_3P and Mn_2P	[17-19]
Fe-Mn-P	Liquidus projection	[9]
	6 vertical sections, at *mass ratio* w_{Fe}:w_{Mn} = 19:1, 9:1, 5:5 and 1:9, and at 6 and 12 wt.%P	[9]
	2 isothermal sections, at 1000 and 800 °C	[20]
	P-activity coefficient, γ_P^{Mn}, in liquid, at 1400 and 1550 °C	[21,22]

Table 3 Thermodynamic description of the Fe-Mn-P system

	Ref.
Liquid (1 sublattice, sites: 1, constituents: Fe,Mn,P)	
$L^L_{Fe,Mn} = (-3950 + 0.489\ T) + (1145)(x_{Fe}-x_{Mn})$	[5]
$L^L_{Fe,P} = (-216603 + 47.028\ T) + (-12490-6.749\ T)(x_{Fe}-x_P) + (+43546)(x_{Fe}-x_P)^2$	[6]
$L^L_{Mn,P} = (-283,000 + 64\ T) + (+70000 - 12.5\ T)(x_{Mn}-x_P)$	O*
$L^L_{Fe,Mn,P} = (+185,000 - 50T)x_{Fe} + (+140,000-50\ T)x_{Mn} + (-80,000)x_P$	O*
bcc (1 sublattice, sites: 1, constituents: Fe,Mn,P)	
$L_{Fe,Mn}^{bcc} = (-2759 + 1.237\ T)$	[5]
$L_{Fe,P}^{bcc} = (-18,2800 + 25.6\ T)$	[1]
$L_{Mn,P}^{bcc} = (-68200)$	O*
$L_{Fe,Mn,P}^{bcc} = (-30,000)$	O*
$Tc^{bcc} = 1043x_{Fe} - 580x_{Mn} + x_{Fe}x_{Mn}(123) - 1100x_{Fe}x_P$	[1]
$\beta^{bcc} = 2.22x_{Fe} - 0.27x_{Mn}$	[5]
fcc (1 sublattice, sites: 1, constituents: Fe,Mn,P)	
$L_{Fe,Mn}^{fcc} = (-7762 + 3.865\ T) + (-259)(x_{Fe}-x_{Mn})$	[5]
$L_{Fe,P}^{fcc} = (-15,1700 + 17\ T)$	[1]
$L_{Mn,P}^{fcc} = (-68,200)$	O*
$L_{Fe,Mn,P}^{fcc} = (-50,000)$	O*
$Tc^{fcc} = -201x_{Fe} - 1620x_{Mn} + x_{Fe}x_{Mn}(-2282-2068(x_{Fe}-x_{Mn}))$	[5]
$\beta^{fcc} = -2.1x_{Fe} - 1.86x_{Mn}$	[5]
cbcc (1 sublattice, sites: 1, constituents: Fe,Mn,P)	
$^\circ G_P^{cbcc} = {}^\circ G_P^{whi} + (+30,000)$	E*
$L_{Fe,Mn}^{cbcc} = (-10,184)$	[5]
$L_{Mn,P}^{cbcc} = (-68,200)$	O*
cub (1 sublattice, sites: 1, constituents: Fe,Mn,P)	
$^\circ G_P^{cub} = {}^\circ G_P^{whi} + (+30,000)$	E*
$L_{Fe,Mn}^{cub} = (-11,518 + 2.819\ T)$	[5]
$L_{Mn,P}^{cub} = (-68,200)$	O*
Fe_3P (2 sublattices, sites: 3:1, constituents: Fe,Mn:P)	
$^\circ G_{Fe:P}^{Fe3P} = 3{}^\circ G_{Fe}^{bcc} + {}^\circ G_P^{whi} + (-184,130 - 14.2902\ T + 8.2245TlnT - 0.007518\ T^2)$	[6][a]
$^\circ G_{Mn:P}^{Fe3P} = 3{}^\circ G_{Mn}^{cbcc} + {}^\circ G_P^{whi} + (-160,000 + 20\ T)$	O*
$L_{Fe,Mn:P}^{Fe3P} = (-50,000 + 20\ T)$	O*
Fe_2P (2 sublattices, sites: 2:1, constituents: Fe,Mn:P)	
$^\circ G_{Fe:P}^{Fe2P} = 2{}^\circ G_{Fe}^{bcc} + {}^\circ G_P^{whi} + (-170,652 + 3.0174\ T + 4.5406TlnT - 0.004306\ T^2)$	[6][a]
$^\circ G_{Mn:P}^{Fe2P} = 2{}^\circ G_{Mn}^{cbcc} + {}^\circ G_P^{whi} + (-164,079 - 39.2175T + 6.6209TlnT + 0.002264\ T^2)$	[19][b]
$L_{Fe,Mn:P}^{Fe2P} = (-85,000 + 50\ T)$	O*
FeP (2 sublattices, sites: 1:1, constituents: Fe,Mn:P)	
$^\circ G_{Fe:P}^{FeP} = {}^\circ G_{Fe}^{bcc} + {}^\circ G_P^{whi} + (-136,020 - 11.6006T + 6.3362TlnT - 0.005343T^2)$	[6][a]
Mn_3P (2 sublattices, sites: 3:1, constituents: Fe,Mn:P)	
$^\circ G_{Fe:P}^{Mn3P} = 3{}^\circ G_{Fe}^{bcc} + {}^\circ G_P^{whi} + (-160,000 + 20T)$	O*
$^\circ G_{Mn:P}^{Mn3P} = 3{}^\circ G_{Mn}^{cbcc} + {}^\circ G_P^{whi} + (-174,743 - 31.1129T + 5.6876TlnT + 0.003525\ T^2)$	[19][b]
$L_{Fe,Mn:P}^{Mn3P} = (-30,000 + 20T) + (+10,000)(y_{Fe} - x_{Mn})$	O*
Mn_3P_2 (2 sublattices, sites: 3:2, constituents: Mn:P)	
$^\circ G_{Mn:P}^{Mn3P2} = 3{}^\circ G_{Mn}^{cbcc} + 2{}^\circ G_P^{whi} + (-301,600 - 73.977\ T + 13.9261TlnT)$	O*
MnP (2 sublattices, sites: 1:1, constituents: Mn:P)	
$^\circ G_{Mn:P}^{MnP} = {}^\circ G_{Mn}^{cbcc} + {}^\circ G_P^{whi} + (-136,715 - 41.322\ T + 7.5542TlnT + 0.001002\ T^2)$	O*

Thermodynamic data of pure components are given by Ref 23 unless not shown in the table. Parameters' values, except for *Tc* and β, are in J/mol

O*—Parameter optimized in this work

E*—Parameter estimated in this work

[a]Function simplified in this work. The reference states of Fe and P have been changed from HSER of Shim et al.[6] to bcc Fe and white P, respectively

[b]Function simplified in this work. The reference states of Mn and P have been changed from cub Mn and P_2-gas of Zaitsev et al.[19] to bcc Mn and white P, respectively

Figures 1 and 2 show the Fe-Mn and Fe-P phase diagrams calculated with the parameters of Huang[5] and of Miettinen and Vassilev,[1] respectively. Figure 3 shows the Mn-P phase diagram optimized in the current study. The agreement with the experimental data is good, as shown by Huang[5] for Fe-Mn, by[1,6] for Fe-P, and in Fig. 3 for Mn-P.

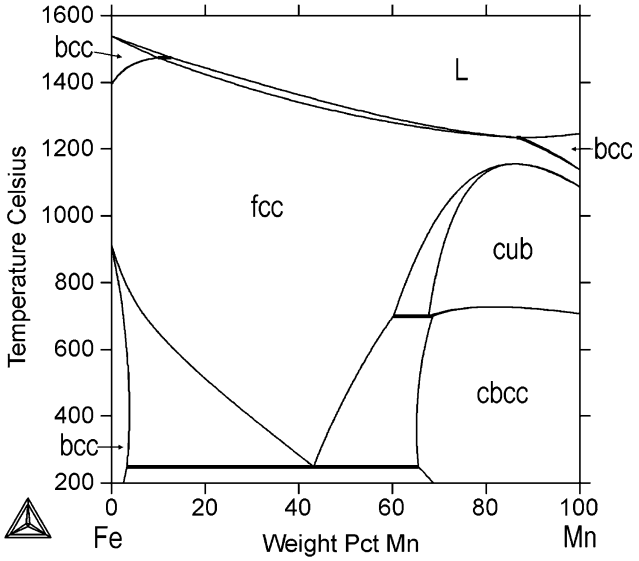

Fig. 1 Calculated with the parameters of Huang[5] Fe-Mn phase diagram

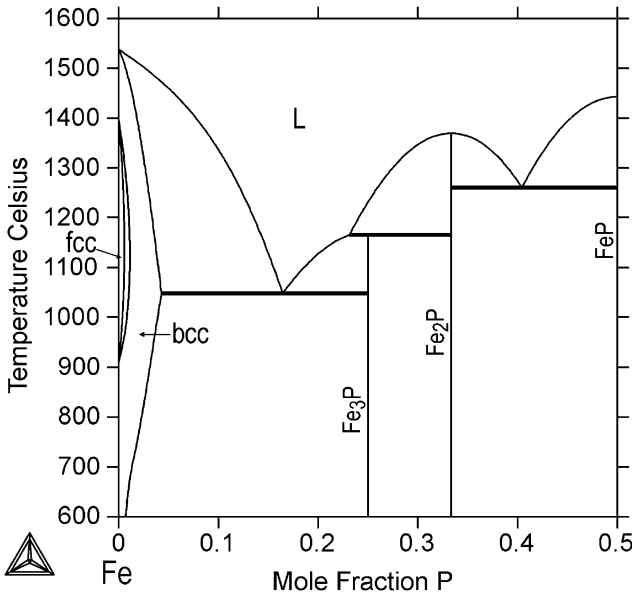

Fig. 2 Calculated with the parameters of Miettinen and Vassilev[1] Fe-P phase diagram. The diagram is identical to that of Shim et al.,[6] excluding minor deviations in the bcc and fcc regions

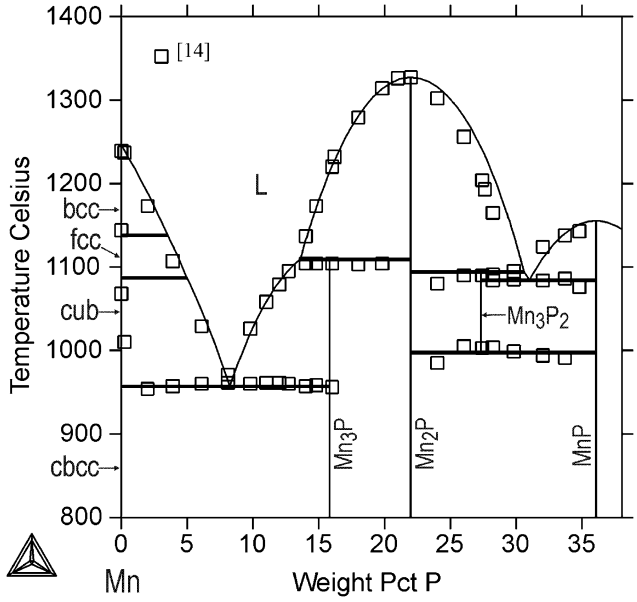

Fig. 3 Mn-P phase diagram, calculated with the parameters optimized in this work, together with experimental data points of Berak and Heumann[14]

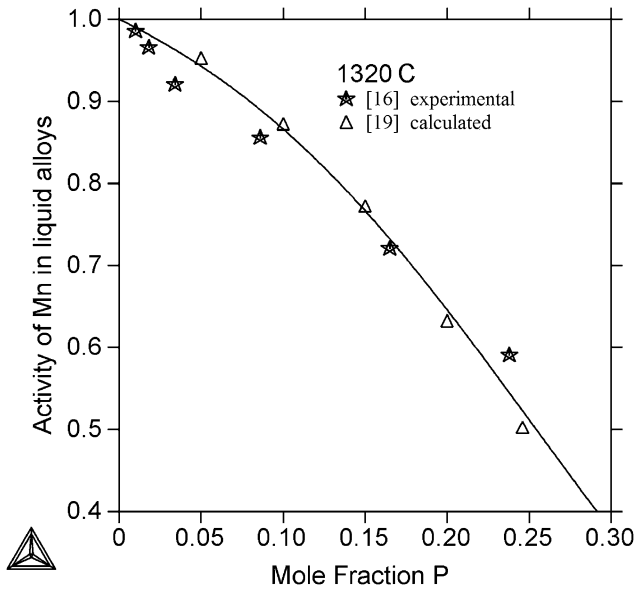

Fig. 4 Calculated activity of Mn in liquid Mn-P alloys at 1320 °C, together with experimental—Batalin et al.[16] and calculated—Zaitsev et al.[19] data points. The reference state used is liquid Mn

Calculated Mn and P activities in liquid alloys at 1320 °C are shown in Fig. 4 and 5, while calculated Gibbs energies of formation of Mn_3P and Mn_2P are plotted in Fig. 6. The agreement with the experimental data of Ref 15-19 is reasonable.

The calculated liquidus projection of the Fe-Mn-P system, together with experimental data points of Vogel and Berak[9] is shown in Fig. 7. It is of worth noting that the manganese content in point U4 (see also Table 4) is inconsistent. This inconsistency was accepted since a stronger stabilization for the cub-phase would have lead to a too extensive primary surface for this phase (see the rounded form of the calculated cub-phase region in Fig. 7), whereas Vogel and Berak[9] presented it as a triangle starting from the binary Mn-P side and approaching point U_4 as a very narrow region. The latter authors[9] suggested one more invariant point, U_5, due to splitting of the fcc phase into Fe-

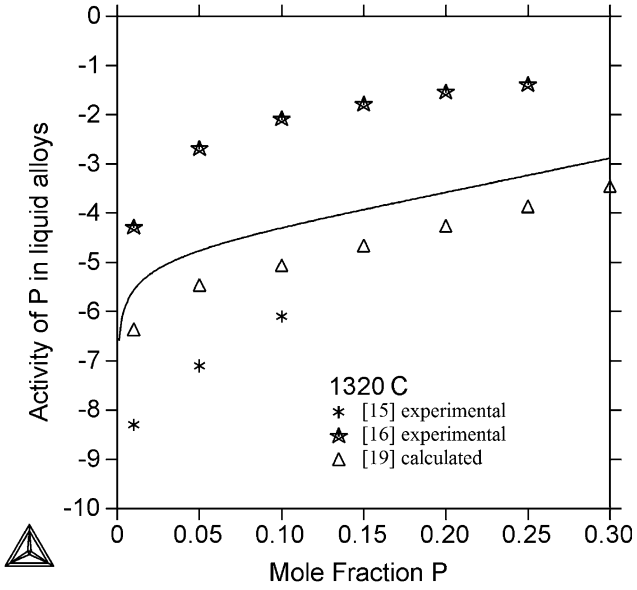

Fig. 5 Calculated in this work P-activity in liquid Mn-P alloys at 1320 °C (solid curve), together with experimental[15,16] and calculated[19] data points. The reference state is P_2-gas

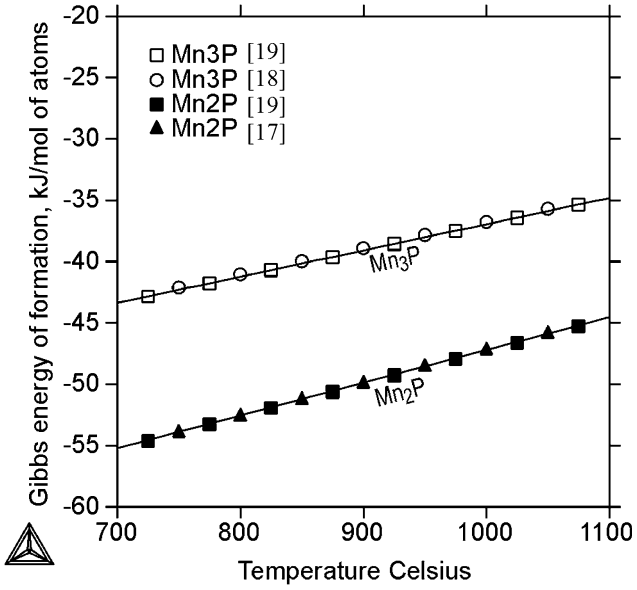

Fig. 6 Calculated in this work Gibbs energies of formation of Mn_3P and Mn_2P, together with experimental data points.[17-19] The reference states used are cub-Mn and P_2-gas

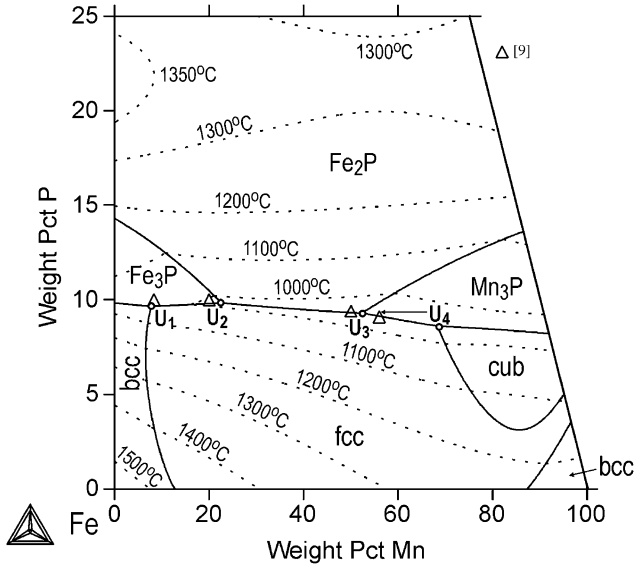

Fig. 7 Calculated liquidus projection of the Fe-Mn-P system, together with experimental data points of Vogel and Berak.[9] Shown also are the calculated liquidus isotherms between 1000 and 1500 °C (dotted lines)

Table 4 Calculated in this study (calc) and experimental (exp) invariant points in the Fe-Mn-P system

Reaction	Code	Temp. (°C)	wt.% Mn in Liq	wt.% P in Liq	Reference
L + bcc = Fe_3P + fcc	U_1	1021	7.7	9.7	calc
		1025	8.3	9.9	exp[9]
L + Fe_3P = Fe_2P + fcc	U_2	981	22.6	9.8	calc
		1015	20	9.9	exp[9]
L + Mn_3P = Fe_2P + fcc	U_3	950	52.3	9.3	calc
		955	50	9.3	exp[9]
L + cub = Mn_3P + fcc	U_4	952	68.4	8.6	calc
		958	56	9.0	exp[9]

rich and Mn-rich fcc phases. This point was ignored in the current work as such splitting has not been observed in the Fe-Mn system.[13]

Calculated vertical and isothermal sections are presented in Figs. 8, 9, 10, 11, 12, 13, 14, and 15, correspondingly. Good agreement of the current calculations with the experimental data of Vogel and Berak[9,20] is observed.

In Fig. 16 the conformity between the calculated and experimental[21,22] P-activity coefficient (γ_P^{Mn}) data in liquid phase has been verified. The agreement is good, however, the temperature dependence of the calculated γ_P^{Mn} values is slightly different from the experimental.

Finally, it is of worth noting that the formation of a liquid phase miscibility gap in the phosphorus-rich corner of the ternary system, at about 600 K, has been predicted. No experimental data is available to confirm the appearance of that gap but this was accepted in the present evaluation, in order to keep the liquid state ternary

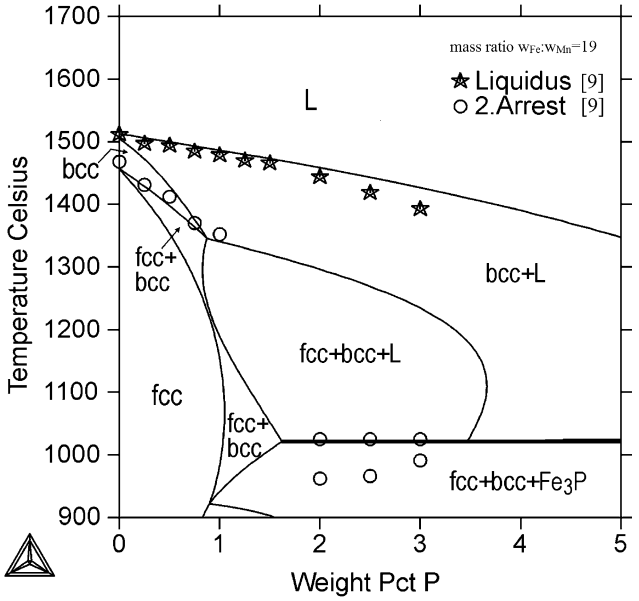

Fig. 8 Calculated vertical section of the Fe-Mn-P system at mass ratio w_{Fe}:w_{Mn} = 19, together with experimental data points of Vogel and Berak[9] (Liquidus—liquidus points, 2. Arrest—thermal arrest data)

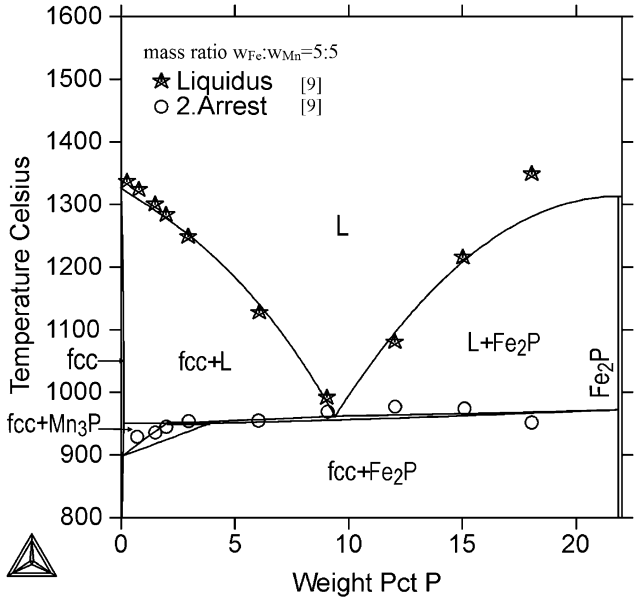

Fig. 10 Calculated vertical section of the Fe-Mn-P system at mass ratio w_{Fe}:w_{Mn} = 5:5, together with experimental data points of Vogel and Berak[9] (Liquidus—liquidus points, 2. Arrest—thermal arrest data)

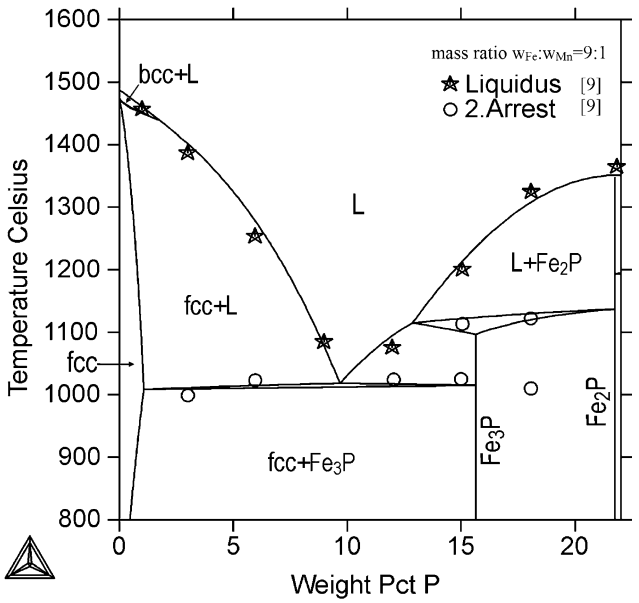

Fig. 9 Calculated vertical section of the Fe-Mn-P system at mass ratio w_{Fe}:w_{Mn} = 9:1, together with experimental data points of Vogel and Berak[9] (Liquidus—liquidus points, 2. Arrest—thermal arrest data)

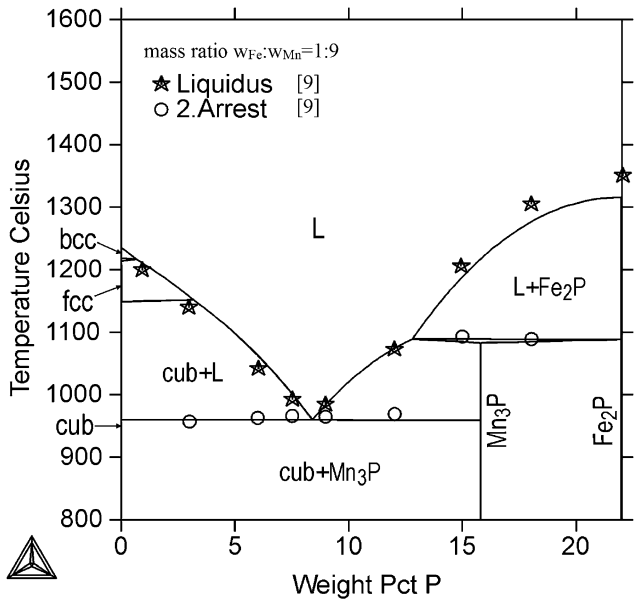

Fig. 11 Calculated vertical section of the Fe-Mn-P system at mass ratio w_{Fe}:w_{Mn} = 1:9, together with experimental data points of Vogel and Berak[9] (Liquidus—liquidus points, 2. Arrest—thermal arrest data)

interaction parameters (Table 3) reasonably simple for the practical calculations at lower phosphorus contents. From theoretical view point[25] such a miscibility gap should be expected, because of the large difference between the atomic radii of the iron and manganese atoms, from one side, and that one of the phosphorus atoms, from other side. Moreover, there is a significant dissimilarity between the chemical character (e.g. the electronegativity) of the phosphorous and the metallic elements (Fe and Mn, in this case).

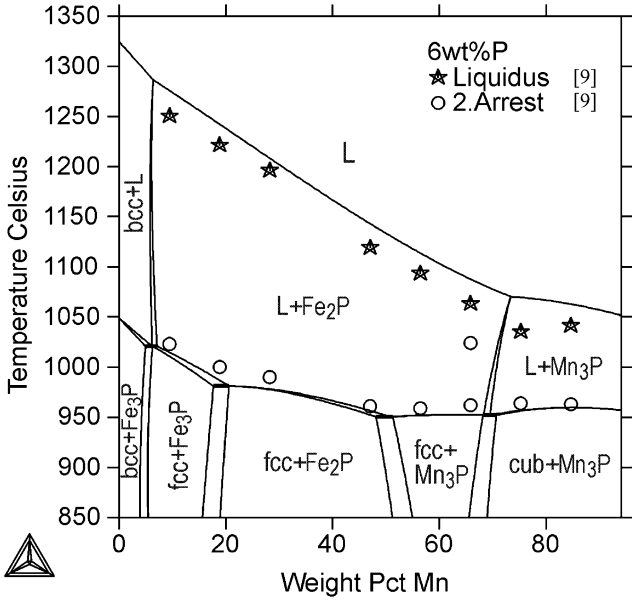

Fig. 12 Calculated vertical section of the Fe-Mn-P system at 6 wt.% P, together with experimental data points of Vogel and Berak[9] (Liquidus—liquidus points, 2. Arrest—thermal arrest data)

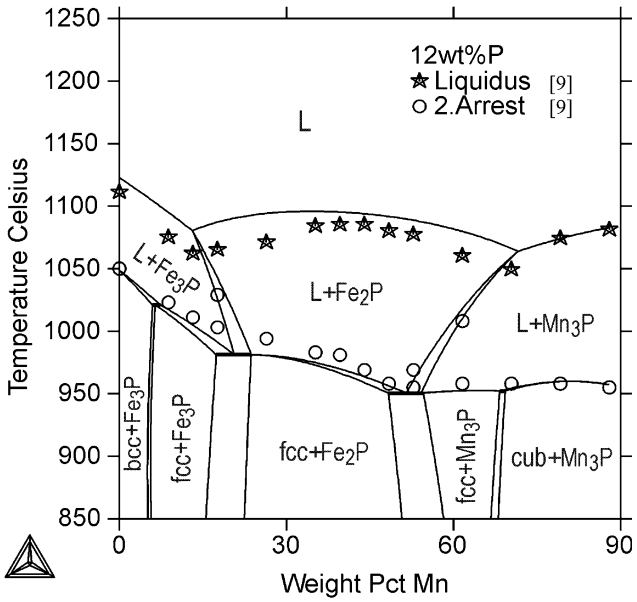

Fig. 13 Calculated vertical section of the Fe-Mn-P system at 12 wt.% P, together with experimental data points of Vogel and Berak[9] (Liquidus—liquidus points, 2. Arrest—thermal arrest data)

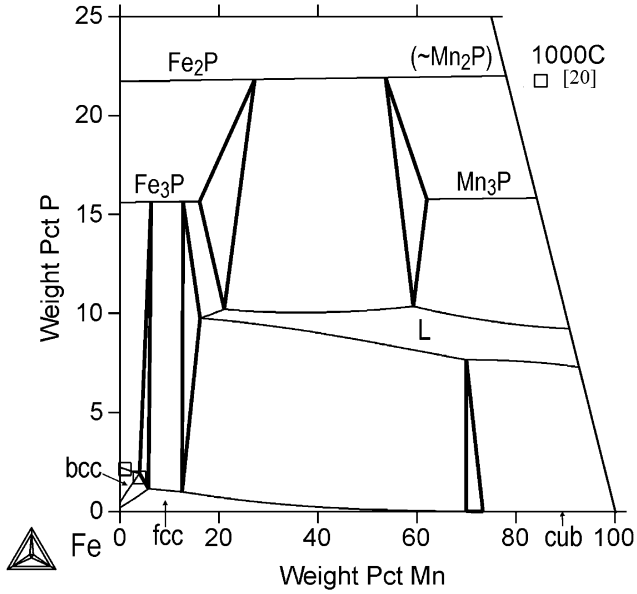

Fig. 14 Calculated isotherm of the Fe-Mn-P system at 1000 °C, together with experimental data points of Kaneko et al.[20]

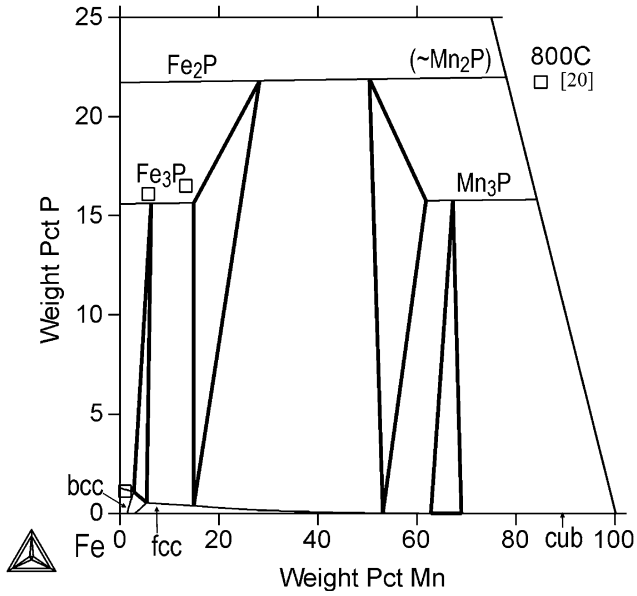

Fig. 15 Calculated isotherm of the Fe-Mn-P system at 800 °C, together with experimental data points of Kaneko et al.[20]

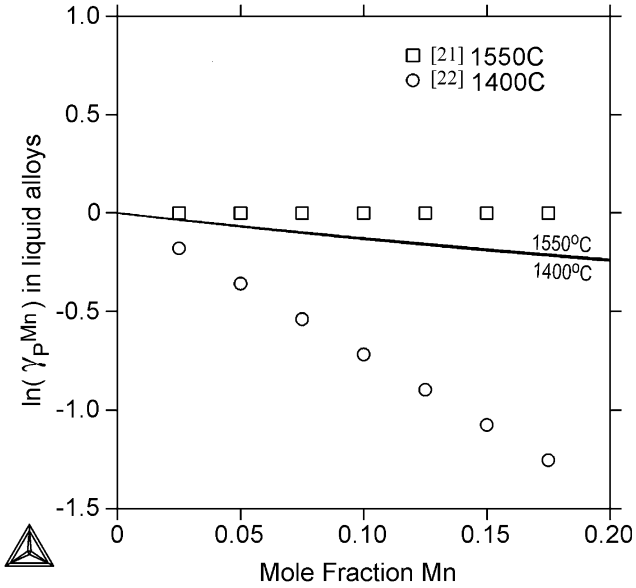

Fig. 16 Calculated P-activity coefficient, γ_P^{Mn}, in liquid Fe-Mn-P alloys at 1400 and 1550 °C, together with experimental data points of Schenck et al.[21] and Ban et al.,[22] respectively

4. Summary

A thermodynamic description has been obtained for the ternary Fe-Mn-P system and its binary sub-system, Mn-P, making use of literature experimental thermodynamic and phase equilibrium data. In the current ternary phase diagram description, twelve phases, i.e., liquid, bcc, fcc, cbcc, cub, Fe_3P (dissolving Mn), Fe_2P (extending to Mn_2P), Mn_3P (dissolving Fe), FeP, Mn_3P_2, MnP and white-P, have been considered. Good or reasonable correlations between the calculated and the experimental thermodynamic and phase equilibrium data have been obtained.

The new Fe-Mn-P description is added as the next member of the thermodynamic database of Fe-X-P systems. No earlier thermodynamic optimization has been found in the open literature for this ternary system.

Acknowledgment

Financial support of the Finnish Funding Agency for Technology and Innovation (TEKES) is gratefully acknowledged by Dr J. Miettinen. The research was carried out as part of the Finnish Metals and Engineering Competence Cluster (FIMECC)'s SIMP program.

References

1. J. Miettinen and G. Vassilev, Thermodynamic Description of Ternary Fe-X-P Systems. Part 1: Fe-Cr-P, *JPED,* 2014, **35**, p. xxx—under printing. doi:10.1007/s11669-014-0314-x
2. J. Miettinen and G. Vassilev, Thermodynamic Description of Ternary Fe-X-P Systems. Part 2: Fe-Cu-P, *JPED,* 2014, **35**, p. xxx—to be printed. doi:10.1007/s11669-014-0315-9
3. J. Miettinen, S. Louhenkilpi, H. Kytönen, and J. Laine, IDS: Thermodynamic-Kinetic-Empirical Tool for Modeling of Solidification, Microstructure and Material Properties, *Math. Comput. Simul.*, 2010, **80**, p 1536-1550
4. J. Miettinen, Thermodynamic Solution Phase Data for Binary Mn-Based Systems, *CALPHAD*, 2001, **25**, p 43-58
5. W. Huang, An Assessment of the Fe-Mn System, *CALPHAD*, 1989, **13**, p 243-252
6. J.-H. Shim, C.-S. Oh, and D.N. Lee, Thermodynamic Properties and Calculation of Phase Diagram of the Fe-P System, *J. Korean Inst. Met. Mater.*, 1996, **34**, p 1385-1393
7. C. Qiu, *Thermodynamic Study of Carbon and Nitrogen in Stainless Steels*. PhD thesis, Royal Institute of Technology, Stockholm, 1993
8. H. Nowotny and E. Henglein, Untersuchung ternärer Legierungen mit Phosphor (Study of Ternary Alloys Containing Phosphorus), *Monatsch. Chem.*, 1948, **79**, p 385-394, in German
9. R. Vogel and J. Berak, Über das System Mangan-Phosphor (The Iron-Phosphorus-Mangenese System), *Arch. Eisenhüttenwes.*, 1952, **23**, p 217-223, in German
10. R. Fruchart, A. Roger, and J.P. Senateur, Crystallographic and Magnetic Properties of Solid Solutions of the Phosphides M2P (M = Cr, Mn, Fe, Co and Ni, *J. Appl. Phys.*, 1969, **40**, p 1250-1257
11. A. Roger, J.P. Senateur, and R. Fruchart, Propriétés cristallographiques et magnétique des solutions solides parmis les phosphides Ni_2P, Co_2P, Fe_2P, Mn_2P et Cr_2P (Crystallographic and Magnetic Properties of Solid Solutions among the Phosphides Ni_2P, Co_2P, Fe_2P, Mn_2P and Cr_2P), *Ann. Chim. (Paris)*, 1969, **4**(2), p 79-91, in French
12. S. Nagase, H. Watanabe, and T. Shinohara, Magnetic Properties of the System Fe_2P-Mn_2P, *J. Phys. Soc. Jpn.*, 1973, **34**(4), p 911-916
13. V. Raghavan, *Phase Diagrams for Ternary Iron Alloys, Part 3*, Indian Institute of Metals, Calcutta, 1988, p 91-99
14. J. Berak and T. Heumann, Über das System Mangan-Phosphor, *Z. Metallkd.*, 1950, **41**(1), p 19-23, in German
15. M.T. Gasik, B.I. Yemlin, and V.F. Gorbachev, *Metallurgy and Chemistry of Carbonite*, Tekhnika Press, Kiev, 1972, p 3
16. G.I. Batalin, V.A. Stukalo and N.Ya. Neshchimenko, Термодинимическая активность фосфора в жидких сплавах марганца с фосфора, (Phosphorous thermodynamic activity in liquid manganese phosphorous alloys) *Украинский Химический Журнал* (*Ukr. Khim. Zh.*), 1977, **43**, p 602-604, in Russian
17. F. Granjean, D.W. Osborn, W.G. Lyon, and H.E. Flotow, Dimanganese Phosphide, Mn_2P: Heat Capacity from 5 to 350 K, Magnetic Entropy, and Thermodynamic Functions to 1300 K, *J. Chem. Thermodyn.*, 1977, **9**, p 549-559
18. Y.E. Lee, Thermodynamics of the Mn-P System, *Metall. Trans. B.*, 1986, **17**, p 777-783
19. A.I. Zaitsev, A.D. Litvina, N.E. Shelkova, Z.V. Dobrokhotova, and B.M. Mogutnov, Thermodynamic Properties of Alloys of Phosphorus with Calcium, Barium, Chromium, Manganese and Iron, *Z. Metallkd.*, 1997, **88**, p 76-86
20. H. Kaneko, T. Nishizawa, K. Tamaki, and A. Tanifuji, Solubility of Phosphorus in α; and γ Iron, *Nippon Kinzoku Gakkai-Si*, 1965, **29**, p 166-170, in Japanese
21. H. Schenck, E. Steinmetz, and H. Gitizad, Die Phosphoraktivität im flussigen Eisen und ihre Beeinflussung durch Nickel, Mangan and Chrom (The Influence of Nickel, Manganese and Chromium on the Phosphorous Activity in Liquid Iron), *Arch. Eisenhüttenwes.*, 1969, **40**, p 597-602, in German

22. S. Ban-Ya, N. Maruyama, and Y. Kawase, Effects of Ti, V, Cr, Mn Co, Ni, Cu, Nb, Mo and W on the Activity of Phosphorus in Liquid Iron, *J. Iron Steel Inst. Jpn.*, 1984, **70**, p 65-72, in Japanese
23. A.T. Dinsdale, SGTE Data for Pure Elements, *CALPHAD*, 1991, **15**, p 317-425
24. J.-O. Andersson, T. Helander, L. Höglund, P. Shi, and B. Sundman, Thermo-Calc & DICTRA, Computational Tools for Materials Science, *CALPHAD*, 2002, **26**, p 273-312
25. G.P. Vassilev, Systematic of Binary Phase Diagrams, Formed by Low-Melting Elements (Bi, Sn, Zn, In) and the Metals of IV-th and V-th Periods, *JMM*, 2005, **41B**, p 79-93